

Biocompatible Heterostructured Nanoparticles for Multimodal Biological Detection

Jin-sil Choi,[†] Young-wook Jun,[†] Soo-In Yeon,[‡] Hyoung Chan Kim,[§] Jeon-Soo Shin,^{*,‡} and Jinwoo Cheon^{*,†}

Department of Chemistry, Yonsei University, Seoul 120-749, Korea, Department of Microbiology, College of Medicine, Yonsei University, Seoul 120-752, Korea, and National Fusion Research Center, Korea Basic Science Institute (KBSI), Daejeon 305-333, Korea

Received September 11, 2006; E-mail: jsshin6203@yumc.yonsei.ac.kr; jcheon@yonsei.ac.kr

During the past decade, inorganic nanoparticles have been utilized as probes and vectors for biomedical applications owing to their enhanced physical properties that arise from nanoscale phenomena.¹ Recently, researchers have begun to explore heterostructured nanoparticles by integrating multiple nanoparticle components into a single nanosystem, and, in particular, advances in the nonhydrolytic colloidal synthesis of nanoparticles have enabled the production of fused inorganic–inorganic hybrid nanostructures such as core–shells and onions,² heterodimers and multimers,³ and dumbbell-type structures.⁴ This protocol produces excellent multicomponent hybrid nanoparticles in terms of size and shape uniformity and single crystallinity, in addition to robust heteroepitaxial inorganic binding between nanoparticulate components. However, these heterostructured nanoparticles cannot be directly utilized for biomedical applications because of their limited water-solubility and poor biocompatibility. Therefore, these nanoparticles require a development of a reliable protocol that addresses these issues without sacrificing their multifunctionalities.

In this paper, we present the development of heterodimer nanoparticles of FePt–Au with multifunctionalities: (i) catalytic effects of FePt for heteroepitaxial Au growth, (ii) high water-solubility and biocompatibility attained through versatile ligand chemistry of Au–S linkages, (iii) Au for chip-based biosensing, and (iv) magnetic resonance (MR) contrast effects of superparamagnetic FePt.

To achieve uniform FePt–Au heterodimer synthesis, the prevention of the nucleation of isolated Au is critical. FePt nanoparticles of 6 nm were synthesized through a transmetalation reaction between Fe⁰ and Pt²⁺ precursors by following a literature method.⁵ When 6 nm FePt nanoparticles were allowed to react with AuCl(PPh₃) in 1,2-dichlorobenzene containing 1-hexadecylamine, under continuous bubbling of 4% H₂/Ar mixture through the solution, the Pt containing nanoparticle seed served as a catalytic surface which activates hydrogen molecules and facilitates the reduction of incoming Au¹⁺ to Au⁰, and the successive growth of Au to the seed resulted in heterodimers of FePt–Au (Figure 1a).⁶ Such a catalytic effect of the FePt seeds is reflected in the decreased temperature required for the formation of Au through the reduction of Au¹⁺ precursor. Without Pt-containing nanoparticle seeds, Au formation required higher growth condition (~150 °C), while it occurred at ~70 °C in the presence of FePt.

Transmission electron microscope (TEM) investigation of the synthesized FePt–Au nanoparticles confirms that our synthetic strategy is effective. Relatively monodispersed heterodimer nanoparticles consisting of a ~6 nm FePt sphere ($\sigma < 8\%$) attached to a ~10 nm Au sphere ($\sigma < 10\%$) are obtained (Figure 1b), while self-nucleated and isolated gold nanoparticles are hardly observed.

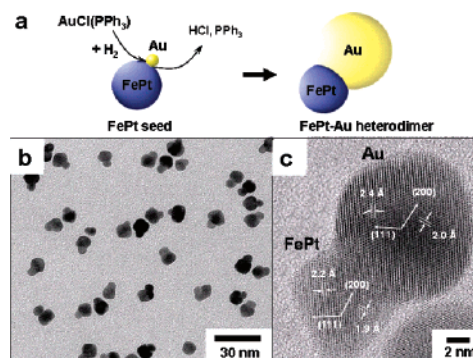


Figure 1. (a) Schematic of FePt–Au heterodimer formation; (b) TEM image and (c) HR-TEM image of FePt–Au heterodimer nanoparticles.

High-resolution TEM (HR-TEM) analyses of a heterodimer show that both monomeric nanoparticle components possess single crystallinity (Figure 1c). Lattice fringes with interplanar spacings of 1.9 and 2.2 Å corresponding to the (200) and (111) planes of face centered cubic (fcc) FePt are clearly observed. On the other hand, as a larger sphere of a heterodimer, lattice fringes with interplanar spacings of 2.0 and 2.4 Å corresponding to the (200) and (111) planes of fcc Au are observed. Diffraction studies including selected area electron diffraction (SAED) and X-ray diffraction (XRD) analyses further confirmed the single crystallinity of heterodimer nanoparticles (see Supporting Information).

We examined magnetic and optical properties of our heterodimer nanoparticles. FePt–Au heterodimers exhibit superparamagnetic behavior with a magnetization value of 52 emu/g (Fe) at 5 T, which is consistent with that of the initial FePt seed nanoparticles (55 emu/g (Fe)). This value is higher than that (40 emu/g (Fe)) of similar sized 6 nm Fe₃O₄ nanoparticles which are widely used as MR probes. Therefore, FePt can be advantageous as highly sensitive probes for MRI. In addition, these heterodimers exhibit a characteristic surface plasmon peak at $\lambda_{\text{max}} = 530$ nm (see Supporting Information).

For biomedical applications, attaining water-solubility and biocompatibility is a prerequisite. The unique structure of our FePt–Au heterodimer nanoparticles is advantageous for such purposes. Since methods for introducing various ligand molecules on Au surfaces through strong Au–S linkages is efficient, the utilization of Au nanoparticles allows for a strong binding of functionally versatile ligands.⁷ We adopted two different types of biocompatible polyethylene glycol ligands with one end composed of dihydroliipoic acid and the other end remaining as –OH (DHLLA-PEG-OH) or modified to an –NH₂ group (DHLLA-PEG-NH₂).⁸ When a mixture of DHLLA-PEG-OH and DHLLA-PEG-NH₂ with a molar ratio of 9:1 was allowed to react with hydrophobic heterodimer nanoparticles, the ligand became strongly bound to the Au nanoparticle surface via chelating bonds of the 1,3-thiol groups (Figure 2a (i)).

[†] Yonsei University.

[‡] College of Medicine, Yonsei University.

[§] Korea Basic Science Institute.

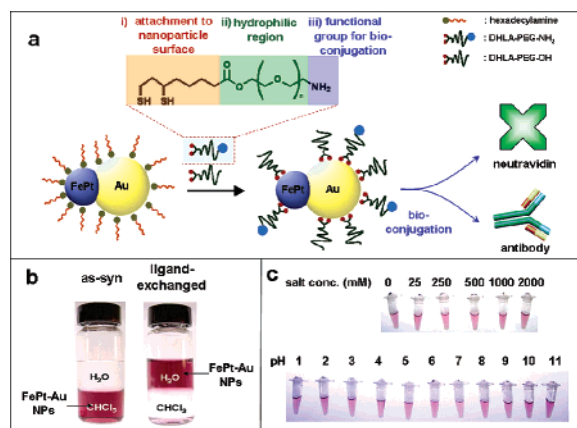


Figure 2. (a) Schematic of capping ligand exchange from hydrophobic to water-soluble FePt–Au; (b) solubility test of as-synthesized (left) and ligand exchanged (right) FePt–Au heterodimer nanoparticles; (c) colloidal stability test of water-soluble FePt–Au heterodimer nanoparticles against salt concentration and pH.

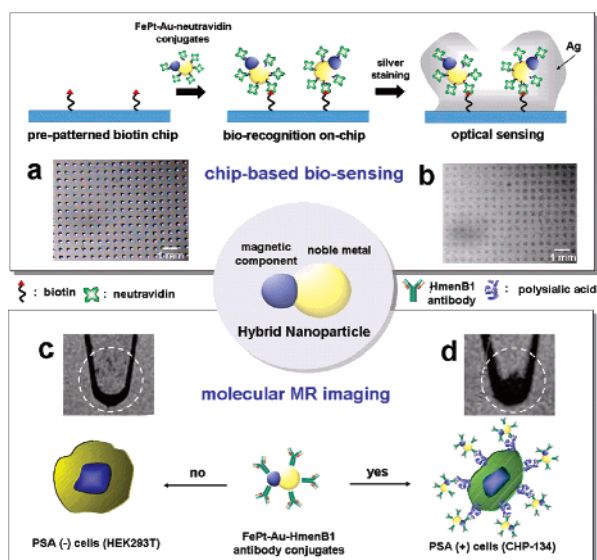


Figure 3. Biochip study and MRI of biological targets. (a,b) Feasibility test of FePt–Au heterodimer nanoparticles as probes for avidin–biotin interactions: (a) prepatterns of biotin and (b) patterns after treatment of FePt–Au. (c,d) In vitro MR imaging of polysialic acids (PSAs) overexpressed on neuroblastoma cells by FePt–Au–HmenB1 antibody conjugates: (c) PSA negative control cells and (d) PSA positive cells.

Hydrophilicity and biocompatibility of nanoparticles can be attained by the polyethylene glycol region of the ligands (Figure 2a (ii)). The amine groups of the DHLA-PEG-NH₂ ligands were used for further bioconjugation (Figure 2a (iii)). After the ligand exchange processes, obtained FePt–Au heterodimers showed excellent colloidal stability in water (Figure 2b), high salt concentration, and various pH conditions within a tested NaCl concentration of 2 M and in the pH range of 1 to 11 (Figure 2c).

We then studied their utility in dual modal-detection applications. We first examined their feasibility as probes for avidin–biotin interaction which is an important biorecognition reaction in chip-based detection. Biotin was patterned in 100 μm × 100 μm squares in which each square was separated by 400 μm (Figure 3a). The substrate was first immersed in a neutravidin-coated FePt–Au (10 μg (Fe)/mL) solution and subsequently treated with a silver-staining solution. In the optical microscopic images, biotin arrays were clearly identified after silver staining while retaining the prepat-

terned size and spacing (Figure 3b). Nonspecific binding on the substrate was not observed at the gap between patterned regions.

We further investigated the applicability of FePt–Au heterodimer nanoparticles for in vitro molecular MR imaging of biological targets. Polysialic acids (PSAs) overexpressed on neuroblastoma cells were used as a case study, where PSA is an important carbohydrate associated with tumor cell growth and metastasis.⁹ We conjugated FePt–Au heterodimers with HmenB1 antibodies which specifically recognize PSAs (Figure 3c).^{9b} The nanoparticle–HmenB1 conjugates were then tested on two different cell lines: target cells (CHP-134) with overexpression of PSA and control cells (HEK293T) without PSA. In the T2* gradient echo images at 9.4 T, while no MR contrast was observed from the PSA negative control cells (Figure 3c), MR contrast effect with significant increase of ~133% in R2* relaxivity (= 1/T2*) was clearly seen from the nanoparticle–HmenB1 conjugate treated PSA positive cells (Figure 3d).

Since a variety of types of heterodimer nanoparticles can be easily fabricated by a combination of different functional nanocomponents (e.g., magnetic, semiconducting, optical) for desired applications, these potentially can serve as a versatile nanoplatform technology for the next generation multimodal biomedical applications including bioseparation, sensing, and imaging.

Acknowledgment. We thank J. M. Oh for TEM, S. H. Kim, and Dr. O. H. Han for MRI (KBSI), and Prof. I.-J. Shin for micropatterning. This work is supported in part by NRL (Grant M10600000255), NCRC (Grant R15-2004-024-02002-0), NCI Center for Cancer Nanotechnology Excellence, KRF (Grant 2004-201-C000501), the BK 21 for Chemistry and Medical Science, and Korea Health 21 R&D of Ministry of Health and Welfare (Grant A050260).

Supporting Information Available: Detailed experimental procedures, XRD, SAED, magnetic hysteresis loop, and UV–vis absorption spectra of FePt–Au heterodimer nanoparticles. This material is available free of charge via the Internet at <http://pubs.acs.org>.

References

- (1) (a) Alivisatos, A. P. *Nat. Biotechnol.* **2004**, *22*, 47. (b) Elghanian, R.; Strohoff, J. J.; Mucic, R. C.; Letsinger, R. L.; Mirkin, C. A. *Science* **1997**, *277*, 1078. (c) Jun, Y.-w.; Huh, Y.-M.; Choi, J.-s.; Lee, J.-H.; Song, H.-T.; Kim, S.-j.; Yoon, S.; Kim, K.-S.; Shin, J.-S.; Suh, J.-S.; Cheon, J. *J. Am. Chem. Soc.* **2005**, *127*, 5732.
- (2) (a) Zeng, H.; Li, J.; Wang, Z. L.; Liu, J. P.; Sun, S. *Nano Lett.* **2004**, *4*, 187. (b) Hirakawa, T.; Kamat, P. V. *J. Am. Chem. Soc.* **2005**, *127*, 3928. (c) Lu, W.; Wang, B.; Zeng, J.; Wang, X.; Zhang, S.; Hou, J. *G. Langmuir* **2005**, *21*, 3684. (d) Lyon, J. L.; Fleming, D. A.; Stone, M. B.; Schiffer, P.; Williams, M. E. *Nano Lett.* **2004**, *4*, 719. (e) Park, J.-I.; Cheon, J. *J. Am. Chem. Soc.* **2001**, *123*, 5743.
- (3) (a) Teranishi, T.; Inoue, Y.; Nakaya, M.; Oumi, Y.; Sano, T. *J. Am. Chem. Soc.* **2004**, *126*, 9914. (b) Yu, H.; Chen, M.; Rice, P. M.; Wang, S. X.; White, R. L.; Sun, S. *Nano Lett.* **2005**, *5*, 379. (c) Shi, W.; Zeng, H.; Sahoo, Y.; Ohulchanskyy, T. Y.; Ding, Y.; Wang, Z. L.; Swihart, M.; Prasad, P. N. *Nano Lett.* **2006**, *6*, 875. (d) Kudera, S.; Carbone, L.; Casula, M. F.; Cingolani, R.; Falqui, A.; Snoeck, E.; Parak, W. J.; Manna, L. *Nano Lett.* **2005**, *5*, 445. (e) Kwon, K.-W.; Shim, M. *J. Am. Chem. Soc.* **2005**, *127*, 10269. (f) Gu, H.; Yang, Z.; Gao, J.; Chang, C. K.; Xu, B. *J. Am. Chem. Soc.* **2005**, *127*, 34.
- (4) Mokari, T.; Rothenberg, E.; Popov, I.; Costi, R.; Banin, U. *Science* **2004**, *304*, 1787.
- (5) Chen, M.; Liu, J. P.; Sun, S. *J. Am. Chem. Soc.* **2004**, *126*, 8394.
- (6) (a) Oudenhuijzen, M. K.; Bitter, J. H.; Koningsberger, D. C. *J. Phys. Chem. B* **2001**, *105*, 4616. (b) Palermo, A.; Williams, F. J.; Lambert, R. M. *J. Phys. Chem. B* **2002**, *106*, 10215.
- (7) Daniel, M.-C.; Astruc, D. *Chem. Rev.* **2004**, *104*, 293.
- (8) (a) Uyeda, H. T.; Medintz, I. L.; Jaiswal, J. K.; Simon, S. M.; Mattoussi, H. *J. Am. Chem. Soc.* **2005**, *127*, 3870. (b) Aronov, O.; Horowitz, A. T.; Gabizon, A.; Gibson, D. *Bioconjugate Chem.* **2003**, *14*, 563.
- (9) (a) Fukuda, M. *Cancer Res.* **1996**, *56*, 2237. (b) Shin, J. S.; Lin, J. S.; Anderson, P. W.; Insel, R. A.; Nahm, M. H. *Infect. Immun.* **2001**, *69*, 3335.

JA066547G